Articles

Synthesis, X-ray Crystal Structure Determination, and Low-Temperature *n*-Hexane Glass Luminescence Studies of $[Cu_{26}(hfac)_{12}(C{\equiv}CR)_{14}]$ (R = *n*-C_4H_9, *n*-C_5H_{11}, *n*-C_6H_{13})

Timothy C. Higgs,* Simon Parsons, Philip J. Bailey, Anita C. Jones, Fiona McLachlan, Andrew Parkin, Alice Dawson, and Peter A. Tasker*,†

Department of Chemistry, The King's Buildings, The University of Edinburgh, West Mains Road, Edinburgh, Scotland, EH9 3JJ, U.K.

Received June 10, 2002

By employment of monoanionic hfac(1,1,1,5,5,5-hexafluoroacetylacetonate) as a "capping ligand", it is possible to modulate the facile accretion of $[\{Cu(C{\equiv}CR)\}_n]$ moieties to yield discrete high-nuclearity Cu(I) clusters of the type $[Cu_{x+y}(hfac)_x(C{\equiv}CR)_y]$. Three more examples of this type of system have been synthesized for alkynyl ligands possessing linear carbon chains ($-C_4H_9{}^n$ to $-C_6H_{13}{}^n$), all with similar formula numbers: $x+y = 26$, $x = 12$, and $y = 14$. These clusters have broad structural similarities to other members of this class of systems, possessing a $Cu_6|Cu_6|Cu_{12(1*)}$-triannular, doubled-layered Cu structure, assembled about a single interplanar linear ($\eta_\sigma{}^1$-RC≡C)$_2$Cu(I) "fulcrum" unit. These systems also possess novel structural features in that the "26th" outermost Cu(I)* ion, required to maintain the charge neutrality of the cluster, is positionally disordered over the periphery of the molecule, inserted into the third Cu-annulus, and therefore effectively acting as a "outersphere" cation. This ion insertion, in two cases, causes significant distortion of the molecule, thus disrupting the complicated mesh of alkynyl-Cu bridging modes within the inner Cu-annuli. The room-temperature (293 K) emission spectrum of $[Cu_{26}(hfac)_{12}(C{\equiv}CC_6H_{13}{}^n)_{14}]$ in *n*-hexane solution exhibits two features, a high-intensity envelope at 344 nm and a lower energy, low-intensity, vibronically structured emission [366, 382, and 399(sh) nm]. Lifetime measurements on these two emissions indicate that they both originate from singlet−singlet transitions. For $[Cu_{26}(hfac)_{12}(C{\equiv}CC_6H_{13}{}^n)_{14}]$ at low temperature, in an *n*-hexane solvent glass, excitation at 280 nm results in two emission bands: one at 350 nm, the other at lower energy, which possesses considerable vibronic fine structure, exhibiting clearly defined maxima at 406, 419, 425, 433, and 448 nm and shoulders at 464 and 482 nm. The absence of the latter feature at 293 K indicates that it is phosphorescent emission, as confirmed by a measured lifetime of 170 ms.

Introduction

The field of Cu(I) alkynyl chemistry is developing rapidly. In part this is because the physicochemical properties of such metal alkynyl compounds which include nonlinear optical activity,[1,2] luminescence,[1,3−21] and molecular conductivity[22] lead to a range of possible commercial applications in electronic and optoelectronic devices[23,24] and in the rapidly evolving field of solution-fabricated nanomaterials.[25,26] To date only a few ho-

† E-mail: p.a.tasker@ed.ac.uk. Fax: (+44)-131-650-6452.

(1) Yam, V. W. W.; Lo, K. K. W.; Fung, W. K. M.; Wang, C. R. *Coord. Chem. Rev.* **1998**, *171*, 17.
(2) Teo, B. K.; Xu, Y. H.; Zhong, B. Y.; He, Y. K.; Chen, H. Y.; Qian, W.; Deng, Y. J.; Zou, Y. H. *Inorg. Chem.* **2001**, *40*, 6794.
(3) Wang, C. R.; Lo, K. K. W.; Fung, W. K. M.; Yam, V. W. W. *Chem. Phys. Lett.* **1998**, *296*, 505.
(4) Yam, V. W. W.; Yu, K. L.; Wong, K. M. C.; Cheung, K. K. *Organometallics* **2001**, *20*, 721.
(5) Yam, V. W. W.; Yu, K. L.; Cheung, K. K. *J. Chem. Soc., Dalton Trans.* **1999**, 2913.
(6) Yam, V. W. W.; Lo, K. K. W.; Wong, K. M. C. *J. Organomet. Chem.* **1999**, *578*, 3.
(7) Yam, V. W. W.; Lo, K. K. W. *Chem. Soc. Rev.* **1999**, *28*, 323.
(8) Yam, V. W. W.; Lee, W. K.; Lai, T. F. *Organometallics* **1993**, *12*, 2383.
(9) Yam, V. W. W.; Lee, W. K.; Cheung, K. K.; Lee, H. J.; Leung, W. P. *J. Chem. Soc., Dalton Trans.* **1996**, 2889.
(10) Yam, V. W. W.; Lee, W. K.; Cheung, K. K.; Crystall, B.; Phillips, D. *J. Chem. Soc., Dalton Trans.* **1996**, 3283.
(11) Yam, V. W. W.; Lee, W. K.; Cheung, K. K. *J. Chem. Soc., Dalton Trans.* **1996**, 2335.
(12) Yam, V. W. W.; Lam, C. H.; Cheung, K. K. *Inorg. Chim. Acta* **2001**, *316*, 19.
(13) Yam, V. W. W.; Fung, W. K. M.; Wong, M. T. *Organometallics* **1997**, *16*, 1772.
(14) Yam, V. W. W.; Fung, W. K. M.; Wong, K. M. C.; Lau, V. C. Y.; Cheung, K. K. *Chem. Commun.* **1998**, 777.
(15) Yam, V. W. W.; Fung, W. K. M.; Cheung, K. K. *J. Cluster Sci.* **1999**, *10*, 37.
(16) Yam, V. W. W.; Fung, W. K. M.; Cheung, K. K. *Organometallics* **1998**, *17*, 3293.
(17) Yam, V. W. W.; Fung, W. K. M.; Cheung, K. K. *Chem. Commun.* **1997**, 963.

10.1021/om020456k CCC: $22.00
Publication on Web 11/20/2002

movalent, homometallic Cu(I) clusters with low nuclearites of 2, 3, 4, or 6 have been structurally characterized.[1,6−13,15−18,20,21,27−38] One significant obstacle in preparing and isolating discrete high-nuclearity Cu(I)-alkynyl complexes has been the ease with which they aggregate indiscriminately, yielding highly insoluble polymeric materials. One tactic to circumvent this problem has been to incorporate "capping ligands" at cluster surfaces to inhibit alkyne-mediated aggregation processes. This approach has mainly used neutral ligands such as phosphine (PPh_3, $Ph_2CH_2PPh_2$, etc.)[1,6,8−13,16−18,20,31,32,38−41] and in just a few cases monoanionic ligands (e.g., 2-$Me_2NCH_2C_6H_4S^-$, 2-$Me_2NC_6H_4^-$).[27−30,36,37] As part of a program to extend this "capping ligand" approach, we surveyed the literature and considered the following design features to enhance the ease of isolation of tractable, discrete Cu(I)-alkynyl cluster compounds:

(i) stoichiometry: [Cu(I)]:[alkynyl]:[capping ligand];

(ii) capping ligand properties: denticity, charge, chelate dimensions, coordination mode (terminal/bridging);

(iii) cluster charge.

Using monoanionic hfac(1,1,1,5,5,5-hexafluoroacetylacetonate) as the capping ligand and controlling the removal of alkyne and hfacH from low-nuclearity intermediates has allowed us to prepare a range of clusters with the general formula $[Cu_{x+y}(hfac)_x(C{\equiv}CR)_y]$ with nuclearities up to 26.[42−45] These fall into two structural classes: (i) multilayered (five examples) and (ii) monolayer (one example) clusters. We describe here the synthesis and characterization of three clusters with the same Cu:hfac:alkynyl stoichiometry, $[Cu_{26}(hfac)_{12}(C{\equiv}CR)_{14}]$, which are structurally similar to the previously reported $[Cu_{26}(hfac)_{11}(C{\equiv}CC_3H_7{}^n)_{15}]$[43] but with differences in the spatial distributions of the ligands. The observation of repeating structural motifs in these clusters allows us to draw some tentative conclusions regarding factors that facilitate the formation of the systems.[44]

Experimental Section

All chemicals were purchased from the Aldrich Chemical Company. *n*-Hexane was distilled over Na/benzophenone/tetraglyme (trace) under nitrogen. Both Et_2O and THF were distilled over Na/benzophenone. All reactions/transfers, etc., were carried out under nitrogen (dried over 4 Å molecular sieves and deoxygenated with BTS catalyst) using standard Schlenk techniques. 1-Hexyne, 1-heptyne, 1-octyne, and 1,1,1,5,5,5-hexafluoropentan-2,4-dione [(hfac)H] were degassed by three freeze/vacuum/thaw cycles. Ultrasound treatments were conducted using an Ultra-Wave U300 bath. Fluorescence spectra were recorded using a Jobin-Yvon FluoroMax photon counting spectrometer. Fluorescence lifetimes were measured using a time-correlated single photon counting system (Edinburgh Instruments) with an instrument response function of 70 ps (fwhm); the excitation source was the third harmonic of a mode-locked Ti:sapphire laser (Coherent Mira).

$[Cu_{26}(hfac)_{12}(C{\equiv}CC_4H_9{}^n)_{14}]$ (Cu_{26}HEX). Into 1-hexyne (6.0 cm^3, 52.2 mmol) was placed Cu_2O (1.64 g, 11.5 mmol) and anhydrous $MgSO_4$ (2.0 g, 16.6 mmol), forming a red suspension. Dropwise addition of hfacH (2.50 cm^3, 17.7 mmol) resulted in an exothermic reaction. After stirring for 18 h *n*-hexane (10 cm^3) was added, the mixture was cannula-filtered, and the solid residue was washed with *n*-hexane (3 × 10 cm^3). The combined yellow-green filtrate and washings were evaporated to dryness in vacuo, giving a dark red oil, which on heating in vacuo at 65 °C for 2 h yielded an orange-red solid. This was suspended in *n*-hexane (40 cm^3) and subjected to ultrasound treatment for 1 h to yield an orange-brown solution containing a microcrystalline bright orange solid, which was collected by filtration, washed with *n*-hexane (2 × 3 cm^3), and dried to give $[Cu_{18}(hfac)_{10}(C{\equiv}CC_4H_9{}^n)_8]$[42] (yield: 2.76 g, 40%), which was imported into a glovebox for storage.

The combined filtrate and washings were reduced to half their original volume in vacuo and set aside. After 5 days ruby-red block crystals had separated. The supernatant liquid was removed by cannula, and the crystals were washed with *n*-hexane (3 cm^3) and dried in vacuo, yielding opaque bright red block crystals of $[Cu_{26}(hfac)_{12}(C{\equiv}CC_4H_9{}^n)_{14}]$ (0.40 g, 4%), which were then imported into a glovebox. Anal. Calcd for $C_{144}H_{138}Cu_{26}F_{72}O_{24}$ C, 32.82; H, 2.64. Found: C, 32.90; H, 2.54. IR (KBr disk, cm^{-1}): 2964, 2936, 2876, 1673, 1639, 1554, 1528, 1460, 1345, 1255, 1208, 1145, 1097, 795, 743, 671, 586, 527.

$[Cu_{26}(hfac)_{12}(C{\equiv}CC_5H_{11}{}^n)_{14}]$ (Cu_{26}HEPT). Into 1-heptyne (7.0 cm^3, 53.4 mmol) was placed Cu_2O (1.263 g, 8.83 mmol) and anhydrous $MgSO_4$ (2.0 g, 16.6 mmol), forming a bright red suspension. Dropwise addition of hfacH (2.50 cm^3, 17.7 mmol) resulted in an exothermic reaction. After stirring for 90 min *n*-hexane (10 cm^3) was added, the mixture was cannula-filtered, and the solid residue was washed with 2 × 5 cm^3

(18) Yam, V. W. W.; Fung, W. K. M.; Cheung, K. K. *Angew. Chem., Int. Ed. Engl.* **1996**, *35*, 1100.
(19) Yam, V. W. W.; Chong, S. H. F.; Wong, K. M. C.; Cheung, K. K. *Chem. Commun.* **1999**, 1013.
(20) Yam, V. W. W.; Choi, S. W. K.; Chan, C. L.; Cheung, K. K. *Chem. Commun.* **1996**, 2067.
(21) Yam, V. W. W. *J. Photochem. Photobiol. A* **1997**, *106*, 75.
(22) Schwab, P. F. H.; Levin, M. D.; Michl, J. *Chem. Rev. (Washington, D.C.)* **1999**, *99*, 1863.
(23) Ma, Y. G.; Che, C. M.; Chao, H. Y.; Zhou, X. M.; Chan, W. H.; Shen, J. C. *Adv. Mater.* **1999**, *11*, 852.
(24) Ma, Y. G.; Chan, W. H.; Zhou, X. M.; Che, C. M. *New J. Chem.* **1999**, *23*, 263.
(25) Tolles, W. M.; Rath, B. B. *Nanomater.: Synth., Prop. Appl.* **1996**, 545.
(26) Tolles, W. M. *Nanotechnology* **1996**, *7*, 59.
(27) van Koten, G.; ten Hoedt, W. M.; Noltes, J. G. *J. Org. Chem.* **1977**, *16*, 2705.
(28) van Koten, G.; Noltes, J. G. *J. Chem. Soc., Chem. Commun.* **1974**, 575.
(29) ten Hoedt, R. W. M.; van Koten, G.; Noltes, J. G. *J. Organomet. Chem.* **1977**, *133*, 113.
(30) ten Hoedt, R. W. M.; Noltes, J. G.; van Koten, G.; Spek, A. L. *J. Chem. Soc., Dalton Trans.* **1978**, 1800.
(31) Song, H. B.; Wang, Q. M.; Zhang, Z. Z.; Mak, T. C. W. *Chem. Commun.* **2001**, 1658.
(32) Osakada, K.; Takizawa, T.; Yamamoto, T. *Organometallics* **1995**, *14*, 3531.
(33) Olbrich, F.; Kopf, J.; Weiss, E. *Angew. Chem., Int. Ed. Engl.* **1993**, *32*, 1077.
(34) Olbrich, F.; Behrens, U.; Weiss, E. *J. Organomet. Chem.* **1994**, *472*, 365.
(35) Naldini, L.; Demartin, F.; Manassero, M.; Sansoni, M.; Rassu, G.; Zoroddu, M. A. *J. Organomet. Chem.* **1985**, *279*, C42.
(36) Knotter, D. M.; Spek, A. L.; Vankoten, G. *J. Chem. Soc., Chem. Commun.* **1989**, 1738.
(37) Knotter, D. M.; Spek, A. L.; Grove, D. M.; Vankoten, G. *Organometallics* **1992**, *11*, 4083.
(38) Gamasa, M. P.; Gimeno, J.; Lastra, E.; Solans, X. *J. Organomet. Chem.* **1988**, *346*, 277.
(39) Diez, J.; Gamasa, M. P.; Gimeno, J.; Aguirre, A.; Garciagranda, S. *Organometallics* **1991**, *10*, 380.
(40) Diez, J.; Gamasa, M. P.; Gimeno, J.; Lastra, E.; Aguirre, A.; Garcia Granda, S. *Organometallics* **1993**, *12*, 2213.
(41) Diez, J.; Gamasa, M. P.; Gimeno, J.; Aguirre, A.; Garcia-Granda, S. *Organometallics* **1997**, *16*, 3684.
(42) Higgs, T. C.; Parsons, S.; Jones, A. C.; Bailey, P. J.; Tasker, P. A. *J. Chem. Soc., Dalton Trans.* **2002**, 3427.
(43) Higgs, T. C.; Parsons, S.; Bailey, P. J.; Tasker, P. A. *Angew. Chem., Int. Ed.* **2002**, *41*, 3038.
(44) Higgs, T. C.; Jones, A.; Parsons, S.; McLachlan, F.; Bailey, P. J.; Tasker, P. A. **2002**, submitted for publication.
(45) Baxter, C. W.; Higgs, T. C.; Jones, A. C.; Parsons, S.; Bailey, P. J.; Tasker, P. A. *J. Chem. Soc., Dalton Trans.* **2002**, in press.

portions of *n*-hexane. The lime-colored filtrate and washings were then evaporated to dryness in vacuo. The resulting dark red "sludge" was heated at 60 °C in vacuo for 4 h, yielding a dark red glass, which was redissolved on gentle heating in 10 cm^3 *n*-hexane and allowed to cool slowly to RT. Over a period of days large dark ruby red crystals separated from the solution; these were collected by cannula-filtration. A second batch of crystals separated from the mother liquor after concentration to half volume. The combined batches were dried in vacuo to give large ruby red opaque block crystals of $[Cu_{26}(hfac)_{12}(C{\equiv}CC_5H_{11}{}^n)_{14}]\cdot 21H_2O$ (yield: 2.30 g, 27%). Anal. Calcd for $C_{158}H_{208}Cu_{26}F_{72}O_{45}$: C, 32.45; H, 3.54. Found: C, 32.44; H, 3.53. IR (KBr disk, cm^{-1}): 2961, 2933, 2862, 1641, 1554, 1529, 1467, 1344, 1257, 1208, 1145, 1098, 795, 744, 671, 586, 527.

$[Cu_{26}(hfac)_{12}(C{\equiv}CC_6H_{13}{}^n)_{14}]$ (Cu_{26}OCT). This compound was made by the same method as $[Cu_{26}(hfac)_{12}(C{\equiv}CC_5H_{11}{}^n)_{14}]$ substituting 1-octyne (8.0 cm^3, 53.4 mmol) for 1-heptyne. Final appearance: Large dark blood-red shiny block crystals (yield: 1.68 g, 20.15%). IR (KBr disk, cm^{-1}): 2958, 2929, 2857, 1672, 1643, 1551, 1528, 1467, 1255, 1207, 1146, 793, 743, 662, 579, 526. Anal. Calcd for $[Cu_{26}(hfac)_{12}(C{\equiv}CC_6H_{13}{}^n)_{14}]$ ($C_{172}H_{194}Cu_{26}F_{72}O_{24}$): C, 36.46; H, 3.45. Found: C, 36.52; H, 3.45.

X-ray Crystallography. The refinement procedures for the crystal structures for the large Cu_{26}OCT, Cu_{26}HEPT, and Cu_{26}HEX systems were complex, with extensive disorder observed in each system, sometimes within the Cu(I) cage. For the purposes of clarity we report each of the refinements individually and exhaustively to preclude any possible ambiguity with respect to the refinement strategies we employed. In each case data were collected with Mo Kα radiation on a Bruker SMART-APEX diffractometer equipped with an Oxford Cryosystems low-temperature device operating at 150 K. Absorption corrections were applied using the program SADABS.[46] Checks for higher space group symmetry were made using the program MISSYM,[47−49] but none was found.

$[Cu_{26}(hfac)_{12}(C{\equiv}CC_6H_{13}{}^n)_{14}]$ (Cu_{26}OCT). The structure of Cu_{26}OCT was solved by direct methods (SHELXTL).[50] Due to the large number of parameters, the Konnert−Hendrickson conjugate-gradient algorithm was used for initial refinement of the structure. Final refinement of the structure used blocked-matrix least-squares against $|F|^2$ (SHELXTL).[50] In common with the hexynyl and heptynyl compounds, there is widespread disorder in the structure. Of the 24 CF_3 groups, 10 were found to be rotationally disordered around the F_3C-C bond, nine in the ratio 50:50 and one 75:25. "Opposite" fluorines were refined with equal anisotropic displacement parameters. No disorder was modeled in the octynyl groups, although the anisotropic displacement parameters for carbon atoms toward the ends of the chains refined to large values. This reflects the probable large dynamic disorder of these groups. Four of the copper-bound carbon atoms were refined isotropically (octynyls B, D, H, and L) due to unrealistic anisotropic behavior. Three areas of electron density were modeled as one disordered Cu(I) ion with relative occupancies 53:30:17.

Diffuse electron density in the structure was treated as described by Van der Sluis and Spek.[51] The number of electrons treated in this way is consistent with four hexane solvent molecules per formula unit.

$[Cu_{26}(hfac)_{12}(C{\equiv}CC_4H_9{}^n)_{14}]$ (Cu_{26}HEX). The structure of Cu_{26}HEX was solved by Patterson methods (DIRDIF)[52] and refined by full-matrix least-squares against $|F|^2$ (SHELXTL).[50] The molecule lies on a crystallographic 32 site, and the structure suffers from extensive disorder. The alkynyl ligand labeled **3** in the tables lies disordered about the crystallographic 3-fold axis. Alkynyls **1** and **2** are also disordered in a way that appears to correlate with the disorder in alkynyl **3**, and so their relative component occupancies were fixed at 2:1. The displacement parameters of the C atoms toward the ends of the chains of these ligands tended to adopt very large (>0.6 $Å^2$) values on free refinement, and it is likely that there is more disorder in these regions than modeled here. Refinements of more elaborate disorder models were unstable and led to little improvement in the agreement indices. The final model presented here has a common isotropic displacement parameter for each chemically equivalent type of C atom in the saturated regions of the alkyl chains; geometry restraints were applied to the bond lengths and angles. Two CF_3 groups are disordered in 70:30 ratio, with the two components related by a 60° ratio about the F_3C-C bond. Geometry restraints were also applied to these moieties, and "opposite" *F*'s were refined with equal anisotropic displacement parameters. The electron density comprising the part-weight atom labeled Cu(6) in the tables could also have been assigned to an oxygen atom, but its contacts were chemically unreasonable. Assignment of this site as $^1/_3$-occupancy Cu(I) ion is also consistent with the disorder in the position of Cu(2)Cu(2′), which makes an unreasonably short contact to Cu(6) when one of its sites is occupied (Cu(2)).

$[Cu_{26}(hfac)_{12}(C{\equiv}CC_5H_{11}{}^n)_{14}]$ (Cu_{26}HEPT). The structure of Cu_{26}HEPT was solved by direct methods (SHELXTL).[50] Due to the overall weakness of the data, a maximum value for 2θ of 45° was used for full-matrix least-squares refinement of the structure against $|F|^2$ (SHELXTL).[50] There is widespread disorder in the structure. The 26th copper atom in the core is modeled as being disordered around a 3-fold axis and also as being present in a 50:50 ratio in the hexynyl/octynyl forms. Of the three crystallographically independent heptynyl moieties, the sixth carbon atom in the chain was refined isotropically, and the very diffuse seventh carbon was unable to be found on the difference map. Hydrogen atom positions were calculated for the first five carbon atoms and for the hfac groups and refined as riding groups. The alkyl chain of heptynyl C was modeled as disordered around a 3-fold axis, and restraints were used on the C−C bond lengths and angles. No disorder was modeled in the CF_3 groups, although the anisotropic displacement parameters for fluorine atoms refined to quite large values, as it was considered that the poor quality of the data did not merit this treatment.

Solid State Structures

Generic Structural Features of Cu_{26}OCT, Cu_{26}HEPT, and Cu_{26}HEX. All three clusters contain 26 Cu(I) ions, 12 hfac and 14 alkynyl anionic ligands. The Cu content of the cluster is encompassed by three radially distributed "annuli" distributed about a single "fulcrum" Cu(I) ion, in a fashion similar to that observed in $[Cu_{26}(hfac)_{11}(C{\equiv}CC_3H_7{}^n)_{15}]$[43] but with some significant differences (Figures 1−4).

The radial annular Cu distribution about the central fulcrum is 6:6:12(1), the outermost annulus containing 12 single-occupancy Cu(I) ions and one (1) disordered over several atomic positions. The Cu content of these clusters can be further subdivided into two "stacked-planes", again similar to $[Cu_{26}(hfac)_{11}(C{\equiv}CC_3H_7{}^n)_{15}]$,[43] each containing 12 Cu ions. This stacked Cu plane molecular architecture is an inevitable consequence of the $\pi+\sigma$ mutually perpendicular bonding vectors of these alkynyl ligands.[44] The center or fulcrum of the

(46) Sheldrick, G. M. *SADABS Program for Empirical Absorption Correction of Area Detector Data*; 1998.
(47) LePage, Y. *J. Appl. Crystallogr.* **1987**, *20*, 264.
(48) Spek, A. L. *J. Appl. Crystallogr.* **1988**, *21*, 578.
(49) Farrugia., L. J. *J. Appl. Crystallogr.* **1999**, *32*, 837.
(50) Sheldrick, G. M. *SHELXTL version 5*; 1995.
(51) Vandersluis, P.; Spek, A. L. *Acta Crystallogr. Sect. A* **1990**, *46*, 194.
(52) Beurskens, P. T.; Beurskens, G.; Bosman, W. P.; Gelder, R. d.; Garcia-Granda, S.; Gould, R. O.; Israel, R.; Smits, J. M. M. *DIRDIF Software System*; 1996.

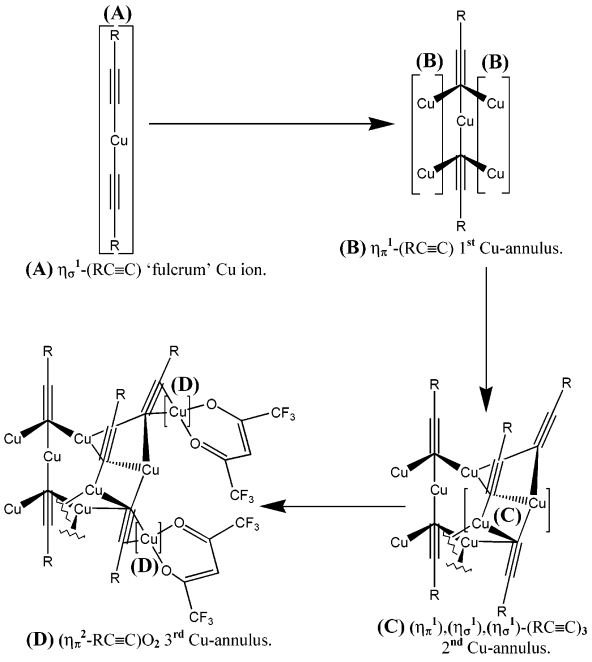

Figure 1. Schematic diagram illustrating the sequential construction of a segment of a [$Cu_{26}(hfac)_{12}(C{\equiv}CR)_{14}$] cluster outward from the fulcrum Cu ion to the third annulus. Bonding to the Cu ions highlighted in parentheses is detailed below each assembly increment.

cluster is occupied by a single Cu ion, situated between the centers of the two Cu_{12} planes, thus acting as a spacer unit, linearly coordinated to two alkynyl ligands via η_σ^1-bonds (Figure 1A). These two alkynyl ligands then further coordinate, via η_π^1-bonds, to several more Cu(I) ions (Figure 1B), from four (Cu_{26}OCT [2.097(8)−2.161(8) Å], Cu_{26}HEX [2.130(2) Å]) to six (Cu_{26}HEPT [2.265(9) Å]), which comprises the first Cu-annulus. For Cu_{26}OCT and Cu_{26}HEX this annulus also contains two atoms that are laterally displaced from the fulcrum alkynyl ligands by 2.495(8)−2.637(9) Å, and these can be considered to be nonbonded, Coulombic interactions. Therefore the first annulus in all three structures contains a total of six Cu ions. The six (Cu_{26}HEPT) and four (Cu_{26}OCT, Cu_{26}HEX) fulcrum-coordinated Cu ions in the first annulus are interlinked with the second and third Cu-annuli via an array of alkynyl ligation modes. Four (Cu_{26}OCT, Cu_{26}HEX) or six (Cu_{26}HEPT) of these Cu ions possess trigonal ligand distributions with one from one of the fulcrum alkynyls and two from 1↔3 interlacing alkynyls (which cross-link the first to the third annuli) via η_σ^1-coordination to one μ_3-alkynyl ligand and η_π^1-coordination to a μ_4-alkynyl ligand, discounting contributions from the 26th disordered Cu ion (Figures 1C and 2−4). The two fulcrum-free, first annular Cu ions in Cu_{26}OCT and Cu_{26}HEX are held in position through two bonding interactions with the network of alkynyl ligands interlacing the second and third Cu-annuli, via η_σ^1-coordination to one μ_3-alkynyl and η_π^1-coordination to a μ_4-alkynyl ligand (Figures 2 and 3). These two pairs of Cu ions are therefore two-coordinate. possessing bowed C−Cu−C bond angles of 145.8(2)° (Cu_{26}HEX) and 144.3(3)°, 147.9(4)° (Cu_{26}OCT). The 12 alkynyl ligands that stabilize the perimeter of the first Cu-annulus additionally interlace the second and third Cu-annuli. The second annulus comprises six

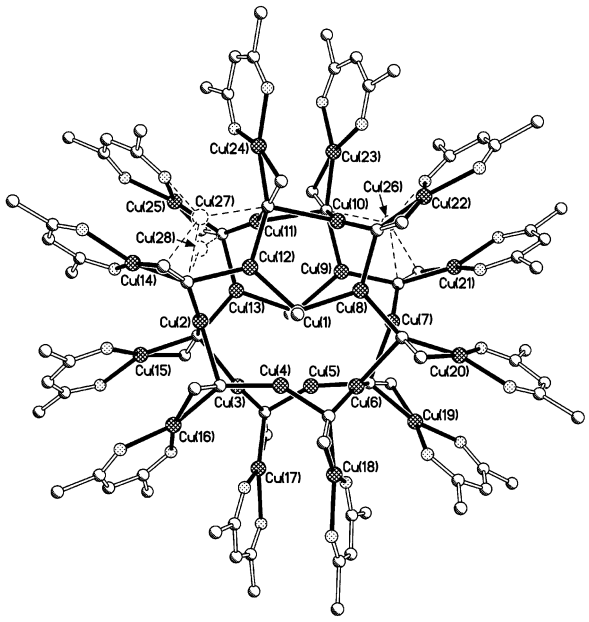

Figure 2. Plot of the [$Cu_{26}(hfac)_{12}(C{\equiv}CC_6H_{13}{}^n)_{14}$] molecule with selected atomic labeling. For the purposes of clarity all possible Cu···Cu bonding, hydrogen and fluorine atoms, and the $-C_6H_{13}{}^n$ groups are omitted. Partial occupancy Cu ions and their associated bonds are dashed.

Cu ions (Figures 2−4), and all are coordinated to three alkynyl ligands, distributed in a trigonal planar array, two being intraplanar with one η_π^1- and one η_σ^1-bond to the μ_4- and μ_3-alkynyl ligands, respectively, and one interplanar, to a μ_4-alkynyl ligand, via a η_σ^1-bond (Figure 1C). This network of alkynyl ligands therefore not only interlaces Cu ions within a plane but also interconnects, and stabilizes, the two stacked Cu_{12} planes. The coordination sphere of each second annulus Cu ion can be summarized thus: (μ_4-)η_π^1-$(C{\equiv}CR)_{intra}$, (μ_3-)η_σ^1-$(C{\equiv}CR)_{intra}$, (μ_4-)η_σ^1-$(C{\equiv}CR)_{inter}$. The third Cu-annulus is comprised of 12 Cu ions each η_π^2-coordinated to, and therefore capping, the radial π-coordination vector of the six alkynyl ligands interweaving each Cu_{12} plane (Figure 1D). These 12 Cu ions are themselves capped by 12 anionic hfac ligands, which therefore prevent polymerization via further accretion of [$Cu_p(C{\equiv}CR)_q$] units. The hfac ligands are each coordinated in a bidentate O_2-donor fashion and distributed in a radial "clockface" arrangement (Figures 1D and 2−4).

The construction of the two Cu_{12} planes via predominantly intraplanar π-coordination and interplanar σ-coordination inevitably aligns the alkynyl ligands parallel to one another in a [7]↑ + [7]↓ fashion, as observed in [$Cu_{26}(hfac)_{11}(C{\equiv}CC_3H_7{}^n)_{15}$],[43] [$Cu_{18}(hfac)_{10}(C{\equiv}CC_4H_9{}^n)_8$],[42] and [$Cu_{18}(hfac)_{10}$ ($C{\equiv}CC_3H_7{}^n)_8$].[44] The 26th Cu(I) ion, which is essential to maintain a charge neutral stoichiometry for the complex, is disordered about several positions at the periphery of the cluster, within the third annulus, over three for Cu_{26}HEX and Cu_{26}OCT and nine for Cu_{26}HEPT. This Cu(I) ion weakly interacts with the ligands exposed at the cluster periphery and therefore behaves effectively as an outersphere cation, being neither totally integrated into nor separated from the main body of the molecule. Details pertinent to the individual disorder patterns are discussed in the specific structural descriptions for these three systems (vide infra).

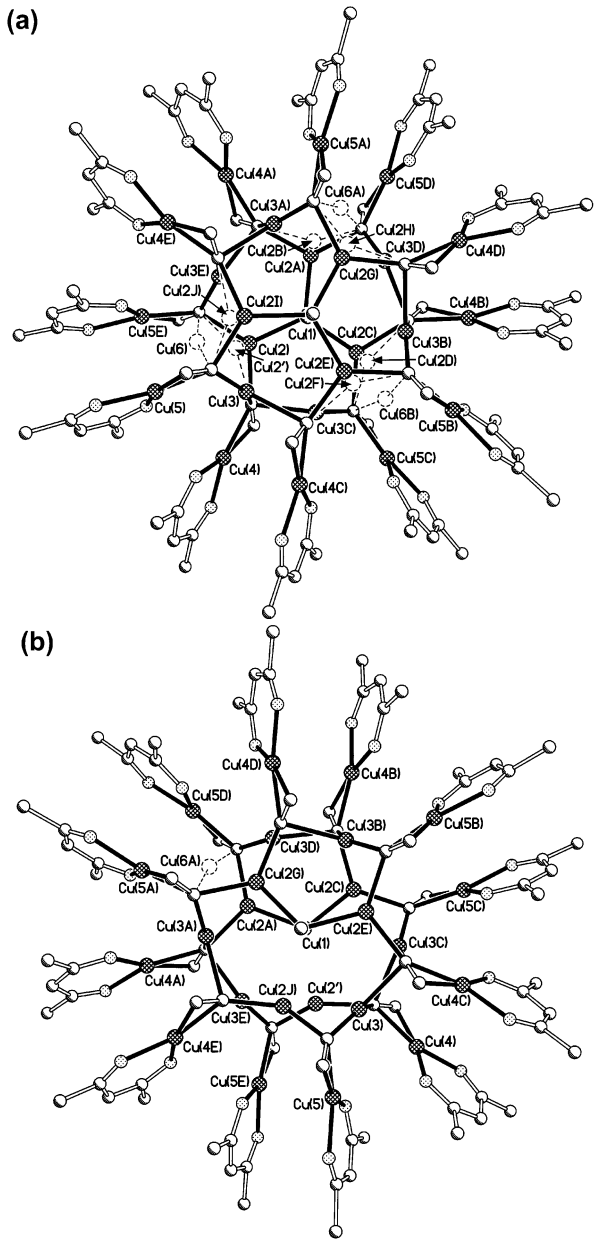

Figure 3. Plot of the $[Cu_{26}(hfac)_{12}(C{\equiv}CC_4H_9{}^n)_{14}]$ molecule with selected atomic labeling. (a) View including all disordered Cu ions (minor occupancy Cu ions and their associated bonds are dashed). (b) View of deconvoluting disorder contributions. For the purposes of clarity all possible Cu···Cu bonding, hydrogen and fluorine atoms, and the $-C_4H_9$ groups are omitted.

Numerous close Cu···Cu contacts, significantly less than the sum of the van der Waals radii for two Cu(I) ions (2.8 Å),[53] are observed in these three systems (Tables 2−4). These distances imply the presence of Cu(I)···Cu(I) [$d^{10}-d^{10}$] closed-shell interactions within the cluster.[54−57] Recent theoretical studies[55] on cuprophilicity have indicated that such interactions have energies as high as 4 kcal mol^{-1}, i.e., comparable to those of hydrogen bonds. These interactions thus make only a small contribution to determining the primary structures of these systems, but may have significant effects on the secondary structure.

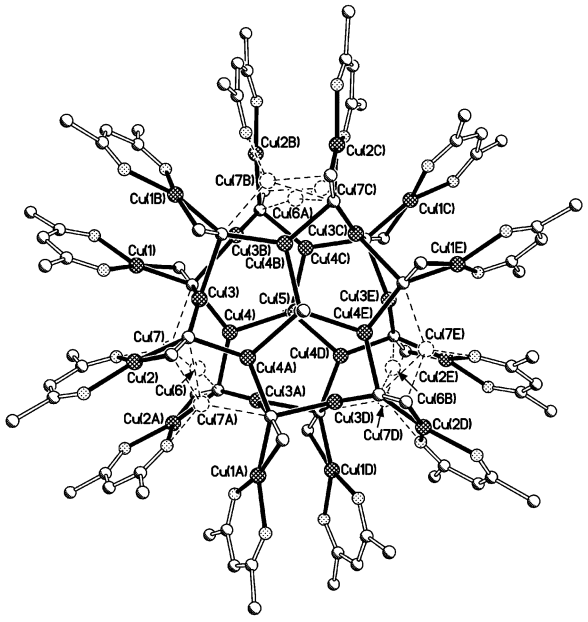

Figure 4. Plot of the $[Cu_{26}(hfac)_{12}(C{\equiv}CC_5H_{11}{}^n)_{14}]$ molecule with selected atomic labeling. For the purposes of clarity all possible Cu···Cu bonding, hydrogen and fluorine atoms, and the $-C_5H_{11}{}^n$ groups are omitted. Partial occupancy Cu ions and their associated bonds are dashed.

$[Cu_{26}(hfac)_{12}(C{\equiv}CC_6H_{13}{}^n)_{14}]$ (Cu_{26}OCT). The asymmetric unit contains one complete molecule of the cluster, therefore containing 26 Cu(I) ions, 12 hfac and 14 octynyl anionic ligands.

The outersphere 26th Cu(I) ion is disordered over three atomic positions with respective occupancies of Cu(26) (0.53890), Cu(27) (0.29423), and Cu(28) (0.16496). Cu(26) and Cu(27) are $\eta_\sigma{}^1$-$(RC{\equiv}C)_1\eta_\pi{}^2$-$(RC{\equiv}C)_1O_1$ and Cu(28) is $\eta_\sigma{}^1$-$(RC{\equiv}C)_2$ coordinated. The Cu(26) and Cu(27) coordination modes are highly anomalous, being dependent on μ_2-O_{hfac} bridging modes, which are rare. In addition, these are the first examples of mixed O/C-$\eta_\sigma{}^1$/C-$\eta_\pi{}^2$-tricoordination to Cu in this class of cluster. It should however be stated that the $\eta_\sigma{}^1$-$(RC{\equiv}C)$ ligands are particularly weakly coordinated, Cu(26) (2.429(8) Å) and Cu(27) (2.403(9) Å), and these were rather arbitrarily designated as being bonds to construct a more "conventional" trigonal coordination geometry.

$[Cu_{26}(hfac)_{12}(C{\equiv}CC_4H_9{}^n)_{14}]$ (Cu_{26}HEX). The crystal lattice is rhombohedral, space group *R*32, the asymmetric unit containing $^1/_6$ of the cluster, the whole being generated by one C_3 axis of rotation and three C_2 rotational axes via a crystallographic 32 symmetry element.

This symmetry leads to complicated positional disorder, primarily located in the first annulus of the Cu cage and the outersphere 26th Cu(I) ion; this has been eluicidated and is described below. The asymmetric unit possesses $4^1/_3$ Cu(I) ions and $2^1/_3$ hexynyl and two hfac anionic ligands. The fulcrum of the cluster consists of a $^1/_6$ occupancy Cu(I) ion, situated on the intersection of the one C_3 and three C_2 axes of the crystallographic 32

(53) Slater, J. C. *J. Chem. Phys.* **1964**, *41*, 3199.
(54) Zuo, J. M.; Kim, M.; O'Keeffe, M.; Spence, J. C. H. *Nature* **1999**, *401*, 49.
(55) Hermann, H. L.; Boche, G.; Schwerdtfeger, P. *Chem. Eur. J.* **2001**, *7*, 5333.
(56) Magnko, L.; Schweizer, M.; Rauhut, G.; Schutz, M.; Stoll, H.; Werner, H. J. *Phys. Chem. Chem. Phys.* **2002**, *4*, 1006.
(57) Che, C.-M.; Mao, Z.; Miskowski, V. M.; Tse, M.-C.; Chan, C.-K.; Cheung, K.-K.; Phillips, D. L.; Leung, K.-H. *Angew. Chem., Int. Ed.* **2000**, *39*, 4084.

Table 1. Crystal Structure Collection Parameters and Data

	Cu_{26}HEX	Cu_{26}HEPT	Cu_{26}OCT
empirical formula	$C_{144}H_{138}Cu_{26}F_{72}O_{24}$	$C_{158}H_{166}Cu_{26}F_{72}O_{24}$	$C_{196}H_{250}Cu_{26}F_{72}O_{24}$
fw	5272.58	5468.95	6010.0
T/K	150(2)	150(2)	150(2)
λ/Å	0.71023	0.71023	0.71073
Bravais lattice	rhombohedral	rhombohedral	monoclinic
space group	$R32$	$R3c$	$P2_1/c$
cell dimens/Å, deg	$a = 22.054(2)$	$a = 22.092(7)$	$a = 25.612(6)$
	$b = 22.054(2)$	$b = 22.092(7)$	$b = 21.047(5)$
	$c = 36.928(5)$	$c = 78.62(4)$	$c = 42.94(1)$
	$\alpha = \beta = 90$	$\alpha = \beta = 90$	$\alpha = \gamma = 90$
	$\gamma = 120$	$\gamma = 120$	$\beta = 100.604(4)$
V/Å^3	15555(3)	33229(21)	22750(9)
Z	3	6	4
ρ/g cm^{-3}	1.689	1.640	1.755
abs/mm^{-1}	2.718	2.548	2.489
$F(000)$		16248	12080
cryst description	red block	red block	red block
cryst size/mm	0.48 × 0.45 × 0.30	0.64 × 0.50 × 0.34	2.5 × 1.0 × 0.51
θ range/deg	1.53−28.94	1.49−22.57	1.14−26.46
no. of reflns collected.	33 624	60 816	142 067
no. of ind reflns	8632	4847	46 561
	[R(int)=0.0348]	[R(int)=0.0771]	[R(int)=0.1823]
abs corr, T_{max}, T_{min}	SADABS[46]	SADABS[46]	SADABS[46]
	0.654, 0.928	0.862, 0.414	0.694, 0.113
H atom placement	geometric	geometric	geometric
no. of data/restraints/params	8632/338/400	4847/557/464	46 561/465/2739
$R_1[\|F\| > 4\sigma(\|F\|)]$	0.0652	0.1245	0.0781
wR_2[all data]	0.2049	0.3527	0.1904
largest peak/e Å^3	0.880	1.602	1.264
largest hole/e Å^3	−0.879	−0.931	−1.169

site, which possesses a coordination number of two from two linearly distributed η_σ^1-hexynyl ligands, thereby separating the two Cu_{12} stacked sheets by approximately 3.77(1) Å. These two hexynyl ligands in turn are apparently μ_3-(η_π^1)$_3$-coordinated to three Cu(I) ions compromising the first annulus of the cluster. These six Cu(I) ions are generated from two disordered within the asymmetric unit of $^2/_3$ [Cu(2)] and $^1/_3$ [Cu(2′)] occupancy, respectively (Figure 3a). The Cu(2) and Cu(2′) subsets of ions are proximate to their respective disorder partners, with Cu(2′) laterally displaced by 0.491(2) Å from Cu(2), toward the periphery of the cluster. Deconvolution of the relative disorder contributions to the apparent structure imposed by the crystallographic symmetry yields a structure strikingly similar to that of the Cu_{26}OCT cluster. One such contributor to the disorder, a deconvolution snapshot, is shown in Figure 3b. The $^1/_3$ occupancy Cu(2′) ion generates two single occupancy Cu ions [Cu(2′) and Cu(2J) in Figure 3b] that are located on opposite Cu_{12} planes. These two Cu ions each has a close contact distance of 2.619(4) Å from the fulcrum Cu(1) coordinating hexynyl, and both therefore can be considered nonbonded to this ligand (i.e., fulcrum-free, vide supra). The $^2/_3$ occupancy Cu(2) ion generates four single-occupancy Cu ions comprised of two pairs located on opposite Cu_{12} planes [Cu(2C), Cu(2D) and Cu(2A), Cu(2B); Figure 3b]. The Cu−C(13/13A)−Cu angles, where C(13) and C(13A) are from the fulcrum hexynyl ligands, are both 116.81(11)°, and the RC≡C(13/13A)−Cu contact distances are 2.130(2) Å. These four C−Cu pairs of atoms can therefore be considered to be coordinated via η_π^1-bonds (vide supra). The fulcrum-Cu and its three surrounding annuli encompass 25 Cu ions of the cluster; the 26th [Cu(6)] is isolated at the periphery of the molecule, being disordered over three C_2 special positions each with an occupancy of $^1/_6$, and again acts as an outersphere cation, achieving an overall charge balanced stoichiometry. It is two-coordinate, to two hexynyl molecules via two long η_σ^1-bonds [Cu(6)−C(12) = 2.249(4) Å, C−Cu(6)−C: 166.3(3)°] as well as being in close proximity to several other Cu ions [Cu(2) 2.291(3) Å, Cu(2′) 1.900(3) Å, Cu(3) 2.357(2) Å, Cu(5) 2.471(2) Å and their proximal symmetry equivalents]. The close contact to Cu(2′) [1.900(3) Å] is chemically unrealistic for a Cu···Cu contact and therefore indicates that Cu(6) is not positioned adjacent to the two atoms symmetry generated from Cu(2′) upon deconvoluting the crystallographic disorder. It is instead positioned adjacent to one pair of the four metal atoms generated from Cu(2) at a more reasonable (though still very short!) Cu···Cu distance of 2.291(3) Å. By happenstance this is the situation observed in the asymmetrical, and therefore unambiguous, Cu_{26}OCT cluster, where the similarly peripherally disordered 26th Cu atom is uniformly situated close to two of the four fulcrum, η_π^1-RC≡C coordinated, first annulus Cu ions. This observation supports the positional assignment of the 26th Cu in Cu_{26}HEX in Figure 3b.

[$Cu_{26}(hfac)_{12}(C{\equiv}CC_5H_{11}{}^n)_{14}$] ($Cu_{26}$HEPT). The crystal lattice is rhombohedral, space group $R3c$, the asymmetric unit containing a $^1/_6$ of the cluster, the whole being generated by one C_3 and three C_2 axes of rotation via a crystallographic 32 site. Thus the asymmetric unit possesses $4^1/_3$ Cu(I) ions and $2^1/_3$ heptynyl and two hfac anionic ligands. This structure suffers from extensive positional disorder, as evinced by its poor R_1 factor of 12.45%, so poor in fact that the several of the heptynyl, $-C{\equiv}CC_5H_{11}{}^n$, chains could not be located and that only the core of the molecule was adequately resolved. Therefore the structural elements will be discussed tentatively with extensive provision made to antecedent [$Cu_{26}(hfac)_{12}(C{\equiv}CR)_{14}$] clusters (Figure 4).

A single Cu(I) ion is contained at the fulcrum position at the exact center of the cluster, located exactly on the

Table 2. Selected Cu−L Bond Distances in $[Cu_{26}(hfac)_{12}(C{\equiv}CC_6H_{13}{}^n)_{14}]$

$[(\eta_\sigma{}^1\text{-}(C{\equiv}C))_2Cu]_{lin}$		Cu(25)−C(2K)	1.975(12)	Cu(26)−C(1N)	2.170(9)
Cu(1)−C(1G)	1.880(8)	Cu(25)−O(254)	1.979(7)	Cu(26)−C(2D)	2.429(8)
Cu(1)−C(1E)	1.913(9)	Cu(25)−O(252)	1.996(7)	Cu(27)−O(252)	2.002(8)
$[(\eta_\pi{}^2\text{-}(C{\equiv}C))O_2Cu]_{trig}$		Cu(25)−C(1K)	2.014(10)	Cu(27)−C(1I)	2.196(10)
Cu(14)−O(144)	1.970(7)	$[(\eta_{\sigma/\pi}{}^{1,1}\text{-}(C{\equiv}C))_3Cu]_{trig}$		Cu(27)−C(1A)	2.200(9)
Cu(14)−C(2A)	1.984(11)	Cu(4)−C(1M)	1.944(10)	Cu(27)−C(2A)	2.403(9)
Cu(14)−O(142)	1.985(7)	Cu(4)−C(1L)	1.970(8)	Cu···Cu (<3.00 Å)	
Cu(14)−C(1A)	2.044(10)	Cu(4)−C(1E)	2.495(8)	Cu(1)−Cu(9)	2.5730(17)
Cu(15)−O(154)	1.956(6)	Cu(5)−C(1B)	1.972(8)	Cu(1)−Cu(12)	2.6458(16)
Cu(15)−C(2J)	1.979(8)	Cu(5)−C(1C)	1.983(9)	Cu(1)−Cu(8)	2.6866(17)
Cu(15)−O(152)	1.980(6)	Cu(5)−C(1G)	2.637(9)	Cu(1)−Cu(13)	2.6957(17)
Cu(15)−C(1J)	2.044(8)	Cu(8)−C(1F)	2.023(8)	Cu(1)−Cu(4)	2.7168(17)
Cu(16)−O(164)	1.961(6)	Cu(8)−C(1H)	2.026(8)	Cu(1)−Cu(5)	2.7694(17)
Cu(16)−O(162)	1.976(6)	Cu(8)−C(1E)	2.145(7)	Cu(2)−Cu(28)	2.397(12)
Cu(16)−C(2L)	2.015(8)	Cu(9)−C(1D)	2.030(8)	Cu(2)−Cu(13)	2.5336(16)
Cu(16)−C(1L)	2.030(8)	Cu(9)−C(1G)	2.097(8)	Cu(2)−Cu(12)	2.6014(16)
Cu(17)−C(2C)	1.957(10)	Cu(9)−C(1N)	2.131(9)	Cu(2)−Cu(3)	2.7243(15)
Cu(17)−O(172)	1.996(6)	Cu(12)−C(1I)	2.046(9)	Cu(2)−Cu(15)	2.7516(16)
Cu(17)−O(174)	2.001(6)	Cu(12)−C(1A)	2.084(8)	Cu(2)−Cu(14)	2.9246(17)
Cu(17)−C(1C)	2.019(8)	Cu(12)−C(1E)	2.112(8)	Cu(3)−Cu(4)	2.5025(17)
Cu(18)−O(184)	1.974(6)	Cu(13)−C(1J)	2.016(8)	Cu(3)−Cu(5)	2.5457(16)
Cu(18)−O(182)	1.978(6)	Cu(13)−C(1K)	2.046(9)	Cu(3)−Cu(16)	2.7873(16)
Cu(18)−C(2M)	1.991(9)	Cu(13)−C(1G)	2.161(8)	Cu(3)−Cu(17)	2.9697(16)
Cu(18)−C(1M)	2.020(8)	$[(\eta_{\sigma/\pi}{}^{1,1}\text{-}(C{\equiv}C))_3Cu]_{trig}$		Cu(4)−Cu(6)	2.5545(16)
Cu(19)−O(192)	1.939(6)	Cu(2)−C(1J)	1.944(8)	Cu(4)−Cu(5)	2.9123(17)
Cu(19)−O(194)	1.970(6)	Cu(2)−C(1A)	1.947(8)	Cu(5)−Cu(6)	2.4977(17)
Cu(19)−C(2B)	1.973(9)	Cu(2)−C(1L)	2.307(8)	Cu(6)−Cu(7)	2.7110(15)
Cu(19)−C(1B)	2.027(8)	Cu(3)−C(1L)	1.925(9)	Cu(6)−Cu(19)	2.7782(16)
Cu(20)−O(204)	1.958(6)	Cu(3)−C(1C)	1.960(11)	Cu(7)−Cu(8)	2.5425(16)
Cu(20)−O(202)	1.990(6)	Cu(3)−C(1J)	2.304(9)	Cu(7)−Cu(9)	2.5701(16)
Cu(20)−C(2F)	1.992(10)	Cu(6)−C(1B)	1.929(8)	Cu(7)−Cu(20)	2.7267(16)
Cu(20)−C(1F)	2.057(8)	Cu(6)−C(1M)	1.949(9)	Cu(7)−Cu(21)	2.9002(16)
Cu(21)−O(212)	1.959(7)	Cu(6)−C(1F)	2.263(9)	Cu(8)−Cu(10)	2.5870(16)
Cu(21)−C(2D)	1.967(9)	Cu(7)−C(1D)	1.934(9)	Cu(9)−Cu(26)	2.302(2)
Cu(21)−O(214)	1.987(6)	Cu(7)−C(1F)	1.964(9)	Cu(9)−Cu(10)	2.6003(16)
Cu(21)−C(1D)	2.060(9)	Cu(7)−C(1B)	2.301(8)	Cu(10)−Cu(26)	2.635(2)
Cu(22)−O(224)	1.977(6)	Cu(10)−C(1H)	1.936(9)	Cu(10)−Cu(23)	2.7831(16)
Cu(22)−C(1H)	1.993(8)	Cu(10)−C(1N)	2.019(9)	Cu(10)−Cu(11)	2.8581(18)
Cu(22)−O(222)	1.999(6)	Cu(10)−C(1I)	2.439(9)	Cu(10)−Cu(22)	2.9680(17)
Cu(22)−C(2H)	2.003(8)	Cu(11)−C(1I)	1.934(9)	Cu(11)−Cu(28)	2.195(10)
Cu(23)−O(232)	1.959(6)	Cu(11)−C(1K)	1.954(11)	Cu(11)−Cu(12)	2.5693(17)
Cu(23)−O(234)	1.979(6)	Cu(11)−C(1N)	2.515(8)	Cu(11)−Cu(13)	2.6122(17)
Cu(23)−C(2N)	2.004(9)	$[(\eta_\pi{}^1\text{-}(C{\equiv}C))_2Cu]_{lin}$		Cu(11)−Cu(27)	2.626(4)
Cu(23)−C(1N)	2.021(8)	Cu(28)−C(1A)	2.136(15)	Cu(11)−Cu(24)	2.7531(16)
Cu(24)−O(244)	1.962(6)	Cu(28)−C(1K)	2.308(17)	Cu(12)−Cu(28)	2.250(15)
Cu(24)−O(242)	1.958(6)	$[(\eta_\pi{}^{1,2}\text{-}(C{\equiv}C))_2OCu]_{trig}$		Cu(12)−Cu(27)	2.271(4)
Cu(24)−C(2I)	1.986(9)	Cu(26)−O(224)	1.983(6)	Cu(13)−Cu(28)	2.454(15)
Cu(24)−C(1I)	2.059(9)	Cu(26)−C(1D)	2.137(8)	Cu(14)−Cu(28)	2.397(10)
				Cu(14)−Cu(27)	2.641(4)
				Cu(21)−Cu(26)	2.652(3)
				Cu(25)−Cu(28)	2.405(13)
				Cu(25)−Cu(27)	2.997(4)

Table 3. Selected Cu−L Bond Distances in $[Cu_{26}(hfac)_{12}(C{\equiv}CC_4H_9{}^n)_{14}]$

$[(\eta_\sigma{}^1\text{-}(C{\equiv}C))_2Cu]_{lin}$		Cu(4)−C(11)	2.027(3)	Cu(2)−Cu(3)4	2.5973(9)
Cu(1)−C(13)	1.887(7)	Cu(5)−O(1B)	1.960(3)	Cu(2)−Cu(3)	2.6184(9)
Cu(1)−C(13)1	1.887(7)	Cu(5)−O(5B)	1.964(4)	Cu(2′)−Cu(6)	1.900(3)
$[(\eta_{\sigma/\pi}{}^{1,2}\text{-}(C{\equiv}C))_3Cu]_{trig}$		Cu(5)−C(22)	1.974(5)	Cu(2′)−Cu(3)	2.4518(16)
Cu(2)−C(13)1	2.1300(15)	Cu(5)−C(12)	2.018(4)	Cu(2′)−Cu(3)4	2.5652(15)
Cu(2)−C(11)	2.058(3)	Cu···Cu (<3.00 Å)		Cu(2′)−Cu(2′)4	2.946(3)
Cu(2)−C(12)4	2.056(4)	Cu(1)−Cu(2)	2.5779(9)	Cu(3)−Cu(6)	2.3567(19)
$[(\eta_{\sigma/\pi}{}^{1,2}\text{-}(C{\equiv}C))_2Cu]_{lin}$		Cu(1)−Cu(2)1	2.5779(9)	Cu(3)−Cu(2′)4	2.5652(15)
Cu(2′)−C(12)4	1.843(4)	Cu(1)−Cu(2)2	2.5779(9)	Cu(3)−Cu(2)4	2.5973(9)
Cu(2′)−C(11)	1.959(4)	Cu(1)−Cu(2)3	2.5779(9)	Cu(3)−Cu(3)1	2.6969(11)
$[(\eta_{\sigma/\pi}{}^{1,1}\text{-}(C{\equiv}C))_3Cu]_{trig}$		Cu(1)−Cu(2)4	2.5779(9)	Cu(3)−Cu(4)	2.7916(7)
Cu(3)−C(12)	1.958(4)	Cu(1)−Cu(2)5	2.5779(9)	Cu(5)−Cu(6)	2.471(2)
Cu(3)−C(11)	1.960(4)	Cu(1)−Cu(2′)	2.923(2)	Cu(6)−Cu(2′)4	1.900(3)
Cu(3)−C(11)1	2.271(4)	Cu(1)−Cu(2′)1	2.923(2)	Cu(6)−Cu(2)4	2.291(3)
$[(\eta_\pi{}^2\text{-}(C{\equiv}C))O_2Cu]_{trig}$		Cu(1)−Cu(2′)3	2.923(2)	Cu(6)−Cu(3)4	2.3567(19)
Cu(4)−O(5A)	1.953(3)	Cu(1)−Cu(2′)5	2.923(2)	Cu(6)−Cu(5)4	2.471(2)
Cu(4)−O(1A)	1.988(3)	Cu(2)−Cu(6)	2.291(3)		
Cu(4)−C(21)	1.977(4)				

crystallographic 32 site and situated equidistant between the two Cu_{12} planes, thus acting as a spacer unit, linearly coordinated to two heptynyl ligands via $\eta_\sigma{}^1$-bonds. These two heptynyl ligands then further coordinate, via $\eta_\pi{}^1$-bonds, to six more Cu ions symmetry generated from a single occupancy Cu(4) ion, these all being encompassed within the first Cu-annulus. Being symmetry equivalent these six Cu(4) ions all possess

Table 4. Selected Cu−L Bond Distances in [$Cu_{26}(hfac)_{12}(C{\equiv}CC_5H_{11}{}^n)_{14}$]

[$(\eta_\sigma{}^1$-(C≡C))$_2$Cu]$_{lin}$		Cu(2)−O(24)	1.965(16)	Cu(3)−Cu(6)	2.337(12)
Cu(5)−C(1C)	1.93(4)	Cu(2)−C(2B)	1.96(2)	Cu(3)−Cu(4)	2.556(4)
Cu(5)−C(1C)2	1.93(4)	Cu(2)−C(1B)	1.975(19)	Cu(3)−Cu(4)1	2.581(3)
Cu(6)−C(1B)	2.31(2)	[$(\eta_{\sigma/\pi}{}^{1,1}$-(C≡C))$_3$Cu]$_{trig}$		Cu(3)−Cu(7)	2.67(3)
Cu(6)−C(1B)1	2.31(2)	Cu(3)−C(1B)	1.95(2)	Cu(3)−Cu(3)2	2.734(5)
[$(\eta_{\sigma/\pi}{}^{1,2}$-(C≡C))$_2O_1$Cu]$_{trig}$		Cu(3)−C(1A)	1.97(2)	Cu(4)−Cu(7)	2.10(4)
Cu(7)−O(24)	1.97(4)	Cu(3)−C(1A)2	2.30(2)	Cu(4)−Cu(6)	2.185(17)
Cu(7)−C(1A)	2.26(4)	Cu(4)−C(1A)	2.048(19)	Cu(4)−Cu(3)1	2.581(3)
Cu(7)−C(1B)1	2.29(4)	Cu(4)−C(1B)1	2.087(19)	Cu(4)−Cu(5)	2.661(3)
Cu(7)−C(2B)1	2.49(4)	Cu(4)−C(1C)	2.265(9)	Cu(5)−Cu(4)3	2.661(3)
[$(\eta_\pi{}^2$-(C≡C))O$_2$Cu]$_{trig}$		Cu···Cu (<3.00 Å)		Cu(5)−Cu(4)2	2.661(3)
Cu(1)−O(12)	1.969(13)	Cu(1)−Cu(3)	2.763(3)	Cu(5)−Cu(4)1	2.661(3)
Cu(1)−O(14)	1.980(14)	Cu(1)−Cu(7)	3.01(3)	Cu(5)−Cu(4)4	2.661(3)
Cu(1)−C(2A)	1.98(2)	Cu(2)−Cu(6)	2.476(16)	Cu(5)−Cu(4)5	2.661(3)
Cu(1)−C(1A)	2.012(19)	Cu(2)−Cu(7)1	2.52(3)	Cu(6)−Cu(4)1	2.185(17)
Cu(2)−O(22)	1.941(14)	Cu(2)−Cu(7)	2.96(4)	Cu(6)−Cu(3)1	2.337(12)
		Cu(2)−Cu(3)	3.006(3)	Cu(6)−Cu(2)1	2.477(16)
				Cu(7)−Cu(2)1	2.52(3)

Table 5. Summary of Electronic Absorption and Luminescence Spectra (Jobin-Yvon FluoroMax Photon Counting Spectrometer) at RT for Cu_{26}HEX, Cu_{26}HEPT, and Cu_{26}OCT (*n*-hexane, λ; nm)[a]

electronic absorption	excitation, λ_{em}, 400 nm	emission,λ_{ex}, 280 nm	emission,λ_{ex}, 340 nm	emission,λ_{ex}, 350 nm
	[$Cu_{26}(hfac)_{12}(C{\equiv}CC_4H_9{}^n)_{14}$] in *n*-Hexane			
241sh(2.57×10^5)	294	344		
286(2.79×10^5)				
329sh(1.49×10^5)	333		368,382(sh),400(sh)	368,382,400(sh)
419sh(3.22×10^4)				
	354(sh)*		379*	391*
	[$Cu_{26}(hfac)_{12}(C{\equiv}CC_5H_{11}{}^n)_{14}$] in *n*-Hexane			
235sh(2.14×10^5)	289	344		
290(1.82×10^5)				
323sh(1.26×10^5)	333		367,380,402(sh)	367,380,402(sh)
417sh(2.50×10^4)				
	355(sh)*			
	[$Cu_{26}(hfac)_{12}(C{\equiv}CC_6H_{13}{}^n)_{14}$] in *n*-Hexane			
234sh(1.88×10^5)	283	344		
290(1.73×10^5)				
329sh(1.03×10^5)	331		366,382,399(sh)	366,382,399(sh)
419sh(2.17×10^4)				
	357*		378*	390*

[a] Column 1, λ; nm (ϵ, $M^{-1}\,cm^{-1}$). Column 2: excitation spectrum in the range 250−390 nm monitoring the emission at 400 nm. Columns 3−5: emission spectra at excitation wavelengths 280, 340, and 350 nm, respectively. The emission signals are correlated to the electronic absorption/excitation bands from which they originate [*solvent Raman bands].

identical (and long) $\eta_\pi{}^1$-RC≡C−Cu bond distances [2.265(9) Å] to the fulcrum heptynyl ligands and so do not exhibit the broken first annulus structure of Cu_{26}HEX and Cu_{26}OCT, instead possessing genuine μ_3-$\eta_\pi{}^1$-fulcrum alkynyl bridging motifs. The three, first annular, Cu(I) ions from each Cu_{12} plane are nearly eclipsed [Cu(4)−C(1C)−C(1CA)−Cu(4A) torsion angle: 23.9°], forming a trigonally distorted prismatic Cu_6 atomic arrangement. As for Cu_{26}HEX and Cu_{26}OCT the 26th Cu ion behaves as an outersphere cation located at the periphery of the cluster. This Cu ion is disordered over two symmetry inequivalent positions, Cu(6) (0.0833) and Cu(7) (0.0833), the former being located on a C_2-axis. Upon symmetry generation via the crystallographic 32 site, a single Cu ion is produced disordered over nine positions. Cu(6) is coordinated via two $\eta_\sigma{}^1$-bonds [2.31(2) Å, C−Cu(6)−C: 168.5(15)°] to two heptynyl ligands from different Cu_{12} planes. Cu(7) is tricoordinated to two heptynyl ligands via a $\eta_\pi{}^2$-bond [2.26(4), 2.29(4) Å] and a very long borderline $\eta_\pi{}^1$-bond [2.49(4) Å] and a μ_2-hfac oxygen atom [1.97(4) Å].

Electronic and Luminescence Spectroscopy. The room temperature luminescence spectra of Cu_{26}HEX, Cu_{26}HEPT, and Cu_{26}OCT in *n*-hexane solution, summarized in Table 5 together with their UV−vis absorptions, are characteristic of this class of cluster, these properties deriving from the numerous (hfac)Cu moieties in each of these clusters.[45]

The luminescence spectra across this series of systems exhibit little variation and so will only be described in detail for [$Cu_{26}(hfac)_{12}(C{\equiv}CC_6H_{13}{}^n)_{14}$] ($Cu_{26}$OCT),[44] a representative example of this type of Cu(I)-alkynyl cluster. Figure 5a indicates that the room-temperature (293 K) emission spectrum of Cu_{26}OCT in *n*-hexane exhibits two significant features. Upon excitation at 240−310 nm, an intense emission with a λ_{max} of 344 nm is observed. The lifetime of this emission was determined to be 2 ns, indicating that the emission results from a spin-allowed transition. On excitation at longer wavelengths (320−350 nm), this strong fluorescence drops off and a much weaker (~5% of 344 nm emisson intensity), vibronically structured, emission band becomes apparent, possessing two maxima at 366 and 382 nm and a shoulder at 399 nm. The lifetime of this emission was 0.9 ns, indicating that this is also due to a spin-allowed transition. Examination of the excitation spectra of Cu_{26}OCT at two different emission wavelengths, 430 and 380 nm (Figure 5a), shows that the intense, higher energy fluorescence results from an absorption band at λ_{max} of 283 nm, and the weaker,

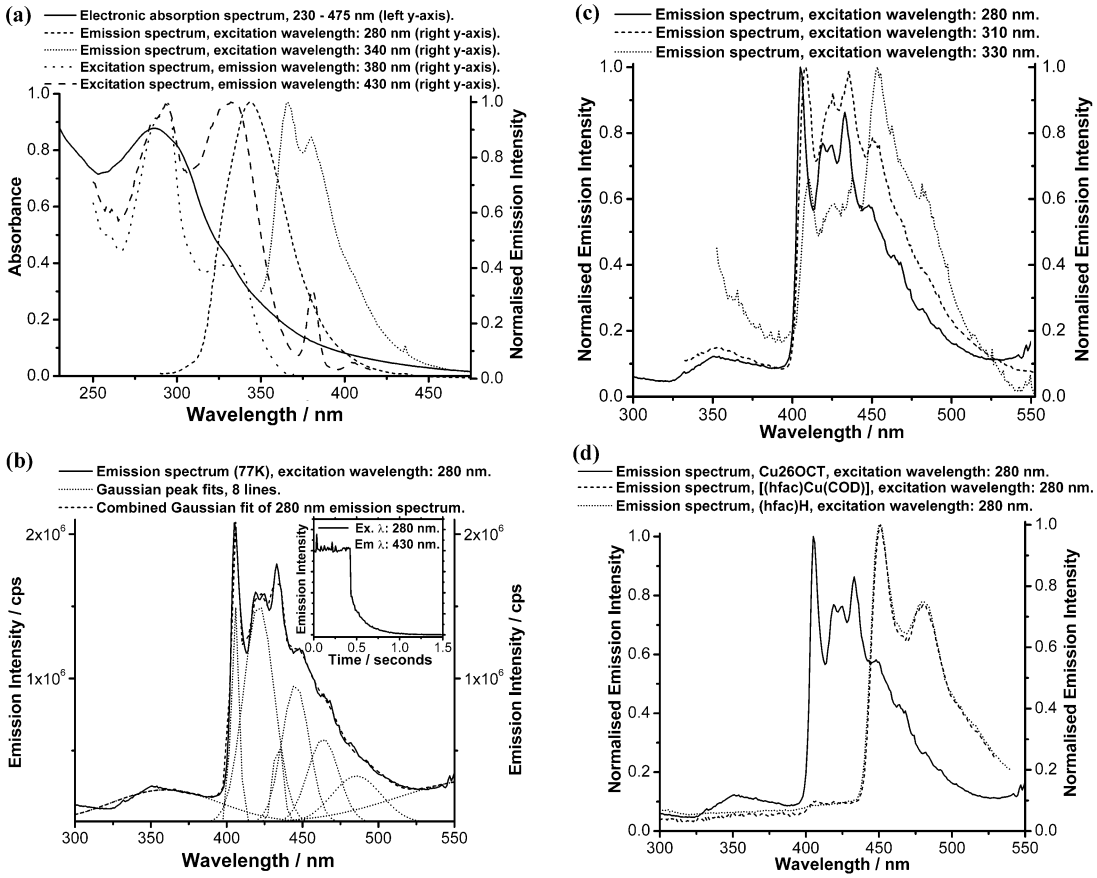

Figure 5. (a) Overlaid electronic absorption, excitation (λ_{em}: 380 and 430 nm) and emission (λ_{ex}: 280 and 340 nm) spectra of Cu_{26}OCT in *n*-hexane, at 293 K. (b) Emission spectrum of Cu_{26}OCT in an *n*-hexane solvent glass, at 77 K, at an excitation wavelength of 280 nm. The spectrum has been deconvoluted assuming Gaussian line shapes using eight peaks. Inset: Long-lived decay of emission intensity at 430 nm; the sharp drop indicates the closure of the excitation shutter. (c) Overlaid emission spectra of Cu_{26}OCT in an *n*-hexane solvent glass, at 77 K, at excitation wavelengths of 280, 310, and 330 nm. (d) Overlaid emission spectra of (hfac)H, [(hfac)Cu(COD)] in ethanol, and Cu_{26}OCT in *n*-hexane at 77 K, all at an excitation wavelength of 280 nm.

lower energy fluorescence band corresponds to an absorption at λ_{max} of 331 nm. Cu_{26}HEX and Cu_{26}HEPT displayed spectral features essentially identical to those described for Cu_{26}OCT, as summarized in Table 5.

The low temperature (77 K) *n*-hexane solvent glass spectra of Cu_{26}OCT[44] are intriguing (Figure 5b). Excitation at 280 nm results in two emission bands. The shorter wavelength, relatively weak band, at 350 nm, corresponds to the 293 K fluorescence band at 344 nm. At longer wavelength, a second, more intense emission envelope is observed. This shows a number of resolvable vibronic bands (Figure 5b), with clearly defined maxima at 406, 419, 425, 433, and 448 nm and shoulders at 464 and 482 nm. Gaussian deconvolution of this complicated emission envelope (Figure 5b) indicates the presence of at least six underlying features. The absence of this long-wavelength emission band at 293 K indicates that it is phosphorescence (spin-forbidden emission). An estimate of the lifetime of this emission was obtained by monitoring the time-dependence of the emission intensity, with a time resolution of 10 ms, after closing a shutter in the excitation beam of the fluorescence spectrometer. A lifetime of 170 ms was measured, confirming a long-lived spin-forbidden excited state. A shorter lived decay component (lifetime <10 ms) was also apparent, but was too short to measure using this rather crude method.

The distribution of intensity within the long-wavelength emission envelope depends on excitation wavelength, as illustrated in Figure 5c. As the excitation wavelength is increased from 280 nm to 330 nm, the emission below 450 nm decreases in intensity and the features above 450 nm become dominant. The relative intensity of the four distinct vibronic bands below 450 nm appears to be essentially independent of excitation wavelength, suggesting that these are all associated with the same electronic transition. Thus, the 400−525 nm emission envelope appears to consist of the overlapping spectra of two different emitting states: one with its origin band at 402 nm and the other with its origin at about 450 nm.

To assist in the assignment of these features, the spectra of the free (hfac)H ligand and a simple monomeric complex, [(hfac)Cu(COD)] (COD: 1,5-cyclooctadiene) were investigated in ethanol at 293 K and in an ethanol solvent glass at 77 K (Figure 5d). (Ethanol was used, as it forms a better glass than hexane at 77 K.) As previously reported by this group,[45] the 293 K high-intensity fluorescence at 344 nm in Cu_{26}OCT is also observed in both (hfac)H and [(hfac)Cu(COD)]; its excitation spectrum coincides with the absorption band at 274 nm of (hfac)H.[58] The lower energy, lower intensity [366, 382, 399sh nm] fluorescence band is also exhibited by both free (hfac)H (weak and poorly re-

solved) and [(hfac)Cu(COD)], indicating that this feature too is hfac-based. No absorption band corresponding to the 331 nm excitation maximum is observed in the electronic spectrum of (hfac)H in ethanol; most likely this is submerged under the intense 274 nm absorption band. Gafney et al.[58] report the phosphorescent emission of (hfac)H, in ethanol at 77 K, to be a vibronically structured envelope in the range 450−575 nm. This has been confirmed by both Halverston et al.[59] for a series of lanthanide complexes of $hfac^-$ and our own measurements of the spectra of free (hfac)H and [(hfac)Cu(COD)] at 77 K (Figure 5d). Therefore, the 450−525 nm component of the Cu_{26}OCT phosphorescent emission can be attributed to the hfac ligands within the cluster, and the measured lifetime of this emission (170 ms) is very similar to those determined for the corresponding phosphorescence of $La(hfac)_3$ (160 ms) and $Eu(hfac)_3$ (250 ms).[59] This leaves the highly structured 400−450 component of the Cu_{26}OCT phosphoresent emission to be identified. Neither (hfac)H nor [(hfac)Cu(COD)] displays emission in this region, indicating that this Cu_{26}OCT emission comes from another component of the Cu_{26}OCT cluster, most likely the Cu(I)-alkynyl core, a conclusion for which there are numerous literature precedents.[1,3−21] The independence of the vibronic intensity distribution of the 400−450 nm emission envelope on excitation wavelength indicates that it originates from a single excited state. This observation and the relatively low energy of the emission suggest that it derives from a delocalized alkynyl-Cu(I) excited state.

Discussion

For the four [$Cu_{x+y}(hfac)_x(C{\equiv}CR)_y$] clusters with a Cu nuclearity of 26 there are many broad structural similarities including a triannular, dual-stacked biplanar arrangement of Cu(I) ions possessing a central, single Cu fulcrum moiety, and a strikingly anisotropic, quasi-tetragonal ligand arrangement with the hfac ligands contained within the equatorial plane and the alkynyl aliphatic chains aligned axially.[43] Closer examination though also reveals several important structural differences within this family of molecules. These variations extend from the fulcrum-Cu to the second Cu-annuli but are most prevalent for the first annulus, which contains six Cu(I) ions. This can either be "totally assembled", for the situation where all six Cu ions are coordinated to one of the two fulcrum alkynyl ligands, or "partially assembled", where two of the six Cu ions are not coordinated to the fulcrum alkynyl ligands. The Cu_{26}HEX and Cu_{26}OCT clusters are definitively of the latter type, whereas the second annulus is complete in Cu_{26}HEPT, and the [$Cu_{26}(hfac)_{11}(C{\equiv}CC_3H_7{}^n)_{15}$] ($Cu_{26}$PENT)[43] is somewhere between, perhaps with a bias toward the latter, with a continuum of bond distances [2.183(5), 2.211(5), 2.226(4), 2.253(4), 2.272(5), 2.363(4) Å]. Five of these, although somewhat long, are clearly bonded $\eta_\pi{}^1$-RC≡C−Cu interactions, but the fifth larger distance is more indicative of a weaker "borderline" interaction. A consistent element in the molecular architecture of these systems which might provide an explanation for the observed solid state structural diversity in this family of molecules is provided by the outersphere inserted 26th Cu ion in Cu_{26}HEX and Cu_{26}OCT. The insertion of this ion into the periphery of these Cu_{26} clusters via transient coordination to the outlying hfac/alkynyl ligands causes these molecules to bulge, thereby causing a profound structural rearrangement in the molecular interior. This concept is illustrated schematically in Figure 6. The 26th Cu approach vector in Cu_{26}HEX and Cu_{26}OCT bisects a pair of transplanar adjacent Cu ions (Figure 6a). This insertion forces the two Cu_{12} planes apart to accommodate this Cu ion (Figure 6a and b). Concomitant with this, the first annulus is distorted from a circular to an elliptical shape (Figure 6a). Two pairs of transplanar Cu ions aligned approximately along the minor elliptical axis remain coordinated to their respective intraplanar fulcrum alkynyl ligands. In contrast, the single pair of transplanar Cu ions aligned along the major elliptical axis are dissociated from the fulcrum alkynyl ligands and are held in position solely by coordinate interactions with the second/third annuli interlacing alkynyl ligands. The reasons for the absence of this signature structural motif in the Cu_{26}HEPT cluster must be approached tentatively due to the poor resolution of this structure (R_1 = 12.45%), which possesses extensive positional disorder. An examination of the final E-map, after convergence of the refinement, indicates that the largest difference peak is only +1.602 e $Å^{-3}$, certainly not large enough to be a $^1/_3$ occupancy Cu ion. This peak is located proximally to the six, first annular, Cu(4) ions (displaced by approximately 0.872 Å). These though have perfectly reasonable thermal parameters for single-occupancy Cu ions. The combination of these observations implies that the first Cu-annulus of Cu_{26}HEPT really does exhibit a complete architecture, a possible explanation for which is provided by the particularly extensive disorder of the 26th outersphere Cu ion over nine positions. An implication that can be derived from this observation is that this ion is particularly poorly integrated into even the periphery of the [$Cu_{25}(hfac)_{12}(C{\equiv}CC_5H_{11}{}^n)_{14}]^-$ anion and

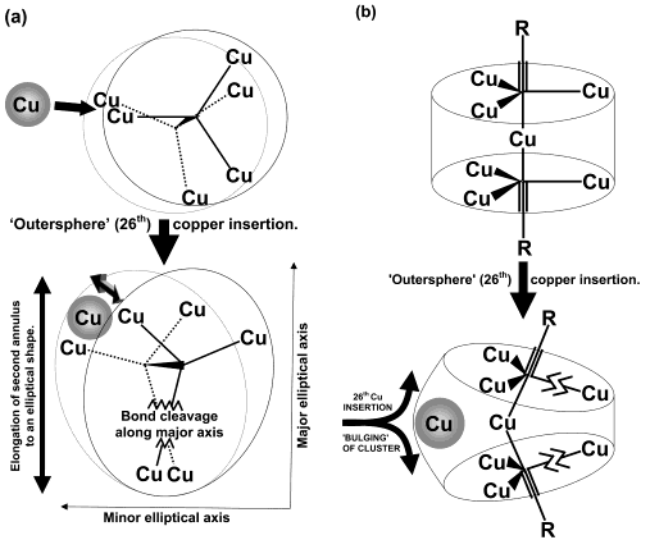

Figure 6. Schematic diagrams of the cluster bulging effect of insertion of the 26th Cu ion into the periphery of the [$Cu_{26}(hfac)_{12}(C{\equiv}CC_4H_9{}^n)_{14}$] and [$Cu_{26}(hfac)_{12}(C{\equiv}CC_6H_{13}{}^n)_{14}$] clusters: (a) apical view; (b) lateral view.

(58) Gafney, H. D.; Lintvedt, R. L.; Jaworiwsky, I. S. *Inorg. Chem.* **1970**, *9*, 1728.
(59) Halverson, F.; Brinen, J. S.; Leto, J. R. *J. Chem. Phys.* **1964**, *40*, 2790.

is thus unable to impart the profound structural modifications of the cluster that are mediated by this outersphere Cu ion in Cu_{26}HEX and Cu_{26}OCT. For asymmetrical Cu_{26}PENT the situation is clearer,[43] for while its classification is slightly ambiguous with one first annular borderline η_π^1-RC≡C−Cu interaction [of 2.363(4) Å], it is most appropriately described as being fully assembled. The reason for it adopting this structural motif is clear from even a cursory examination of the periphery of this molecule, which has developed a distinctive, and to date unique, bud structure to accommodate the 26th outersphere Cu cation. The accommodation of this totally discrete, ordered microstructure on the periphery of the main cluster body causes a radical redistribution of the anionic ligand ratio within this complex to 11 × (hfac):15 × (pentynyl). In contrast, the attachment of this bud onto, and not into, the cluster periphery ultimately causes considerably less disruption of the internal Cu-cage structure, specifically with respect to the dislocation of the two Cu_{12} planes.

Acknowledgment. We would like to thank Stephen Boyer of the Computing and Engineering Department of the University of North London for performing microanalyses. We would also like to thank Chris Baxter for supplying 77 K emission spectra of (hfac)H and [(hfac)Cu(COD)] in an ethanol solvent glass. This work was supported by Avecia, Seiko-Epson Corporation, and EPSRC funding, which is gratefully acknowledged.

Supporting Information Available: This material is available free of charge via the Internet at http://pubs.acs.org.

OM020456K